

## Supplementary Information

### **Universally Applicable RNA Membrane-based Microneedle System for Transdermal Drug Delivery**

Dajeong Kim<sup>1</sup>, Hyejin Kim<sup>1</sup>, Peter C. W. Lee<sup>2,\*</sup> and Jong Bum Lee<sup>1,\*</sup>

<sup>1</sup> Department of Chemical Engineering, University of Seoul, Seoul 02504, South Korea  
Tel: +82-2-6490-2372; Fax: +82-2-6490-2364; Email: jblee@uos.ac.kr

<sup>2</sup> Department of Biomedical Sciences, University of Ulsan College of Medicine, Asan Medical Center, Seoul 05505, South Korea  
Tel: +82-2-3010-2799; Fax: +82-2-2045-4249; Email: pclee@amc.seoul.kr

\* To whom correspondence should be addressed.

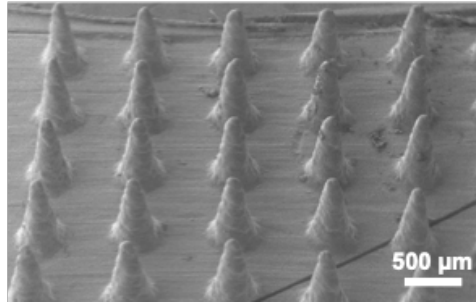


**Fig. S1** SEM image of the 3D-printed scaffold MN array with 42 needles, revealing uniform synthesis of conical MNs on the cuboid scaffold.

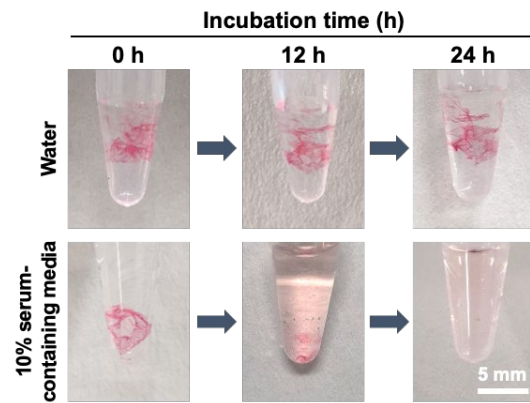


**Fig. S2** Stability of RNA membrane in water or 10% serum-containing media. RNA membrane exhibited high stability in water and selective segmentation in the presence of nuclease. For stability analysis, RNA membrane was incubated in water or 10% FBS-containing RPMI 1640 medium (Gibco, 11835-030) at 37°C for 24 h.

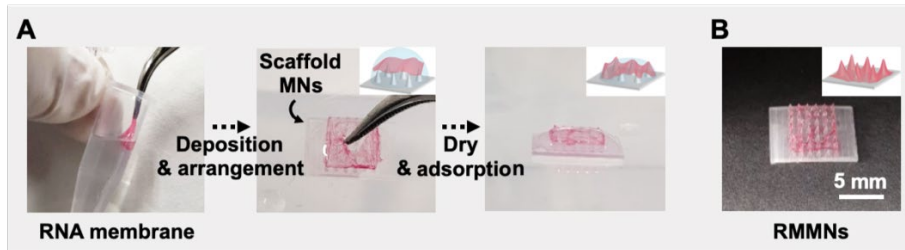


**Fig. S3** Synthesis of RMMN via water-based coating. (A) The RNA membrane was deposited onto the wet scaffold MNs ( $500 \mu\text{m} \times 1500 \mu\text{m}$  in  $W \times H$ ) using a tweezer. The membrane was further aligned using a tweezer for full coverage of the array. With the overnight air-drying process, the RNA membrane was physically adsorbed on the surface along with the conical shape as the water evaporates. (B) The resulting RMMNs show the successful coating of RNA membrane.

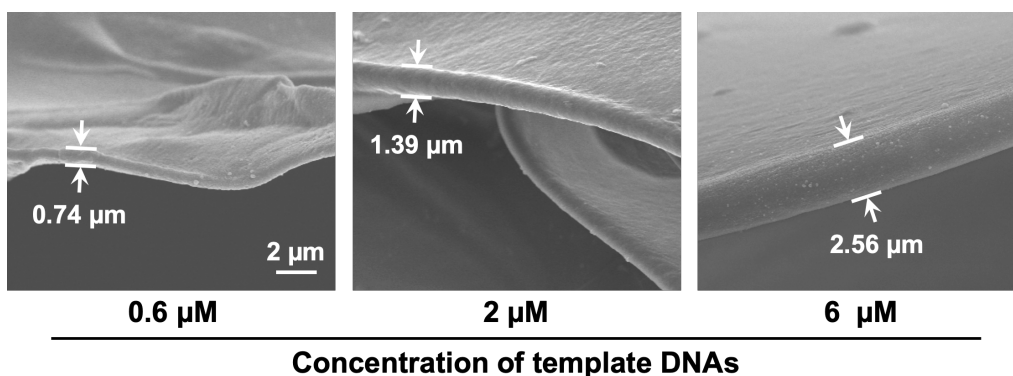


**Fig. S4** Manipulation of thickness of RNA membrane by modifying the concentration of template DNAs. The evaporation rate decreased as the concentration of RNA transcripts in the solution increases via raising the circular DNAs, and the thicker layer could be fabricated. Three different concentrations of circular DNAs (0.6 μM, 2 μM or 6 μM) were used as template DNAs to control the thickness of RNA membrane. The thicknesses were analyzed using ImageJ software.

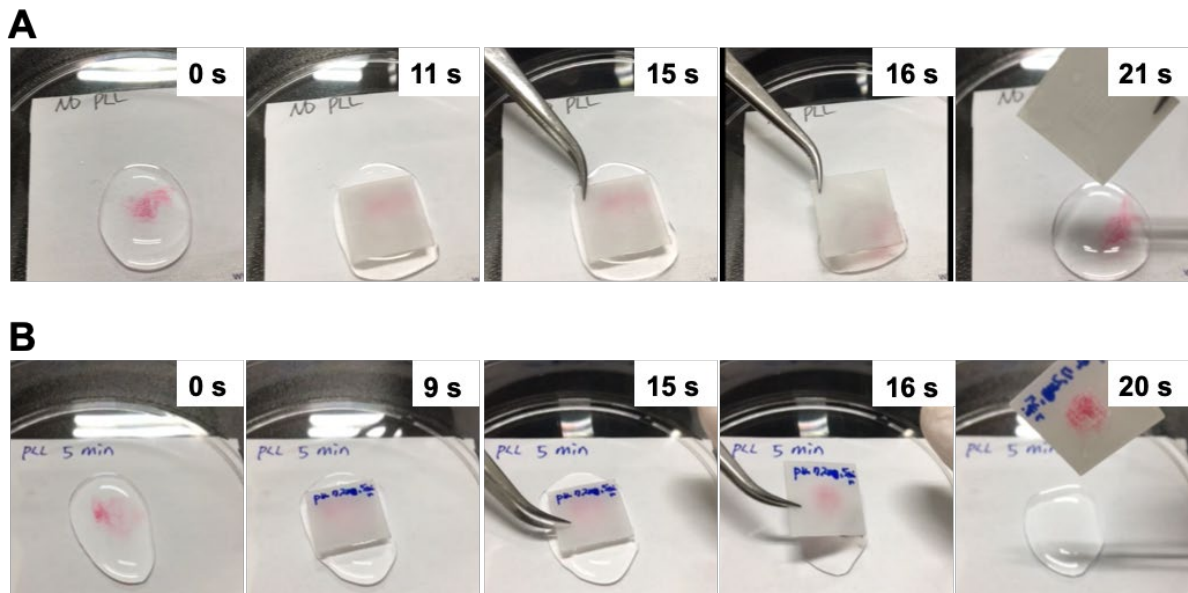


**Fig. S5** Enhanced adsorption by ionic interaction. Digital images of uncoated MN (A) and PLL-coated MN (B) in close contact with the RNA membrane. PLL (1  $\mu\text{g}$ ) was dropped onto the MNs for 5 min and washed with nuclease-free water to prepare PLL-coated MNs. Negatively charged RNA membrane was attracted to PLL-coated MN by electrostatic interaction, while uncoated MN failed to attract the RNA membrane.

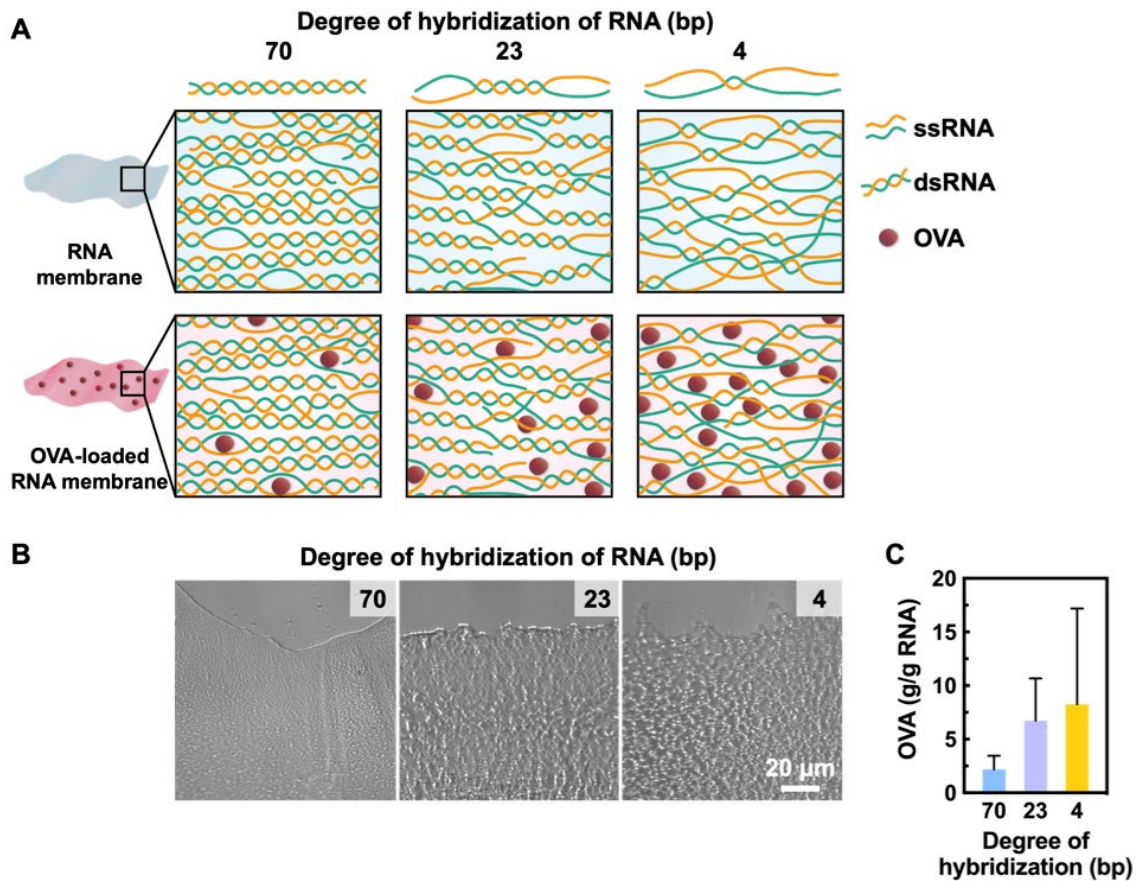


**Fig. S6** Manipulation of internal porosity of RNA membrane. (A) Schematic illustration showing the microscopic spacing between RNA molecules is depending on the degree of hybridization. (B) Digital images showing the macroscopic porosity of RNA membranes made up of different hybridization lengths of RNA. (C) Loaded amount of OVA (g per g RNA membrane), indicating that the loading amount of OVA molecules increased as the degree of hybridization decreased.

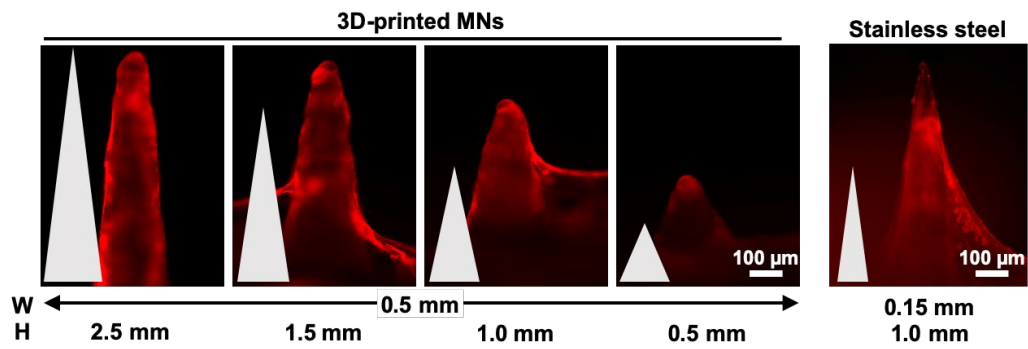


**Fig. S7** Fluorescence images of Gel Red-stained RMMNs from MNs with indicating width and height, showing the successful coating of RNA membrane regardless of sharpness. The MNs were designed to have 0.5 mm of width and height of 0.5, 1.0, 1.5 or 2.5 mm, respectively.



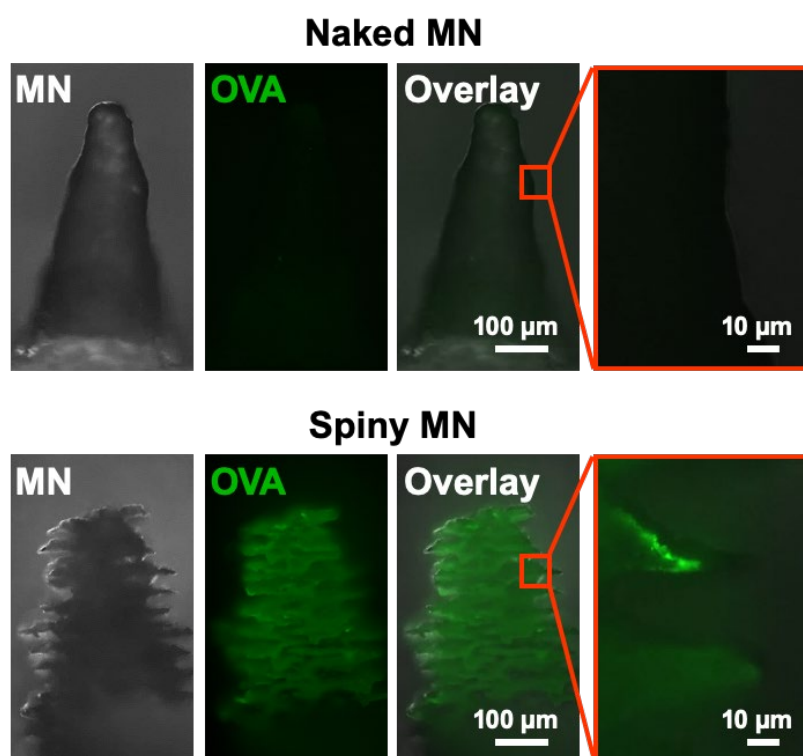


**Fig. S8** Fluorescence microscopy images of the naked MN (top) or spiny MN (bottom) after incubation with Alexa 488-conjugated OVA solution. The spiny MNs were prepared by briefly sonicating the conical MNs. Then, bare or spiny MNs were loaded with OVA by soaking MNs in Alexa 488-conjugated OVA solution (0.1 mg/ml). After 2 h of incubation, the resulting MNs were washed and observed with fluorescence microscopy, indicating efficient encapsulation of OVA into spiny MN.

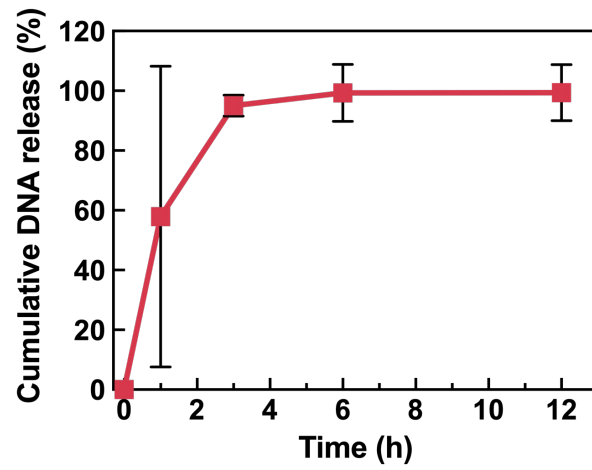


**Fig. S9** The cumulative release profile of DNA from CpG-DNAP-RMMNs in PBS solution (n=3). Data are represented as mean  $\pm$  standard deviation (SD).

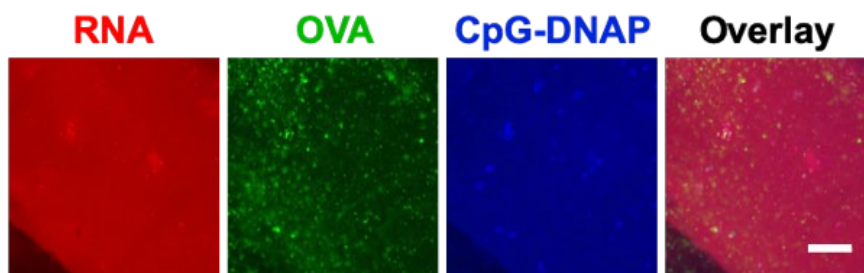


**Fig. S10** Fluorescence microscopy images of CpG-DNAP-incorporated RM pre-loaded with OVA, revealing the colocalization of all components (scale bar: 50  $\mu$ m). The CpG-DNAP was labeled with AMCA-6-dUTP (0.02 mM, Jena Bioscience) during RCA process. Red: Cy5-labeled RNA membrane, green: Alexa 488-conjugated OVA, blue: AMCA-labeled CpG-DNAP.

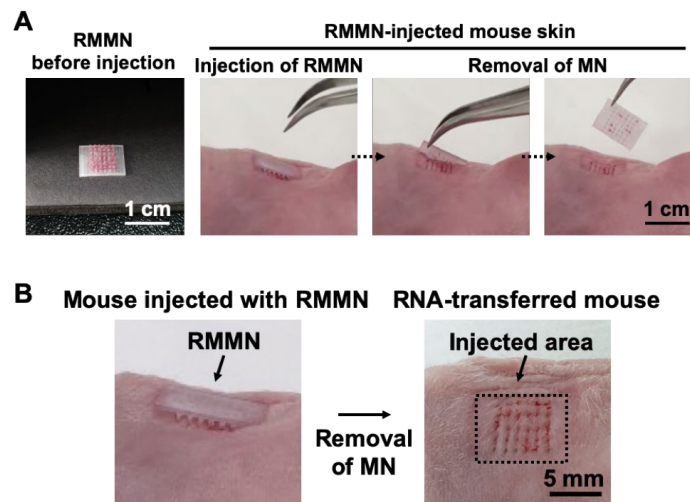


**Figure S11.** *In vivo* transfer analysis of RNA membrane. (A) RMMN was successfully injected into the mouse skin. After the 20 min treatment of RMMN followed by removal of MN, RNA membrane was detached from MN and remained at the injected site. (B) Top view showing the transfer of RNA membrane in an array.

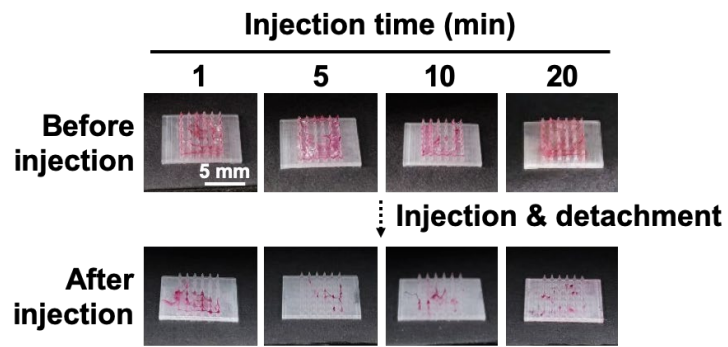


**Fig. S12** *In vivo* RNA transfer test with varying injection time. Most of the RNA was transferred to the mouse skin when treated over 5 min, while 1 min treatment showed inefficient transfer.

**Table S1.** Mechanical properties of printing material for the MNs (Visijet M3 Crystal) supplied by 3D Systems Incorporation.<sup>1</sup>

Properties	Tensile strength	Tensile modulus	Elongation at break	Flexural strength	Heat distortion temperature
Visijet M3 Crystal	42.4 MPa	1463 MPa	6.83%	49 MPa	56°C

**Table S2.** DNA sequences for the synthesis of the RNA membrane. Blue regions in sense and anti-sense strands are complementary to each other. Red regions in both strands have binding sites for T7 promoter DNA.

DNA strands (Length)	Sequence (5'– 3')
T7 promoter for T7 RNA polymerase (20 nt)	TAA TAC GAC TCA CTA TAG GGA T
Linear DNA for sense strand (92 nt)	Phosphate - ATA GTG AGT CGT ATT AGC GAC CGA GTT GCT CTT GCC GTT TTA GAG CTA GAA ATA GCA AGT TAA AAT AAG GCT AGT CCG TTA TCA ACA TCC CT
Linear DNA for anti-sense strand (92 nt, 70 bp hybridization with sense strand)	Phosphate - ATA GTG AGT CGT ATT AGT TGA TAA CGG ACT AGC CTT ATT TTA ACT TGC TAT TTC TAG CTC TAA AAC GGC AAG AGC AAC TCG GTC GCA TCC CT

**Table S3.** DNA sequences for fabricating RNA membranes with different porosity. Red regions in both strands have binding sites for T7 promoter DNA. Hybridization sites with 23 bp-RNA membrane and 4 bp-RNA membranes are shown in green and orange, respectively.

DNA strands (Length)	Sequence (5'– 3')
T7 promoter for T7 RNA polymerase (20 nt)	TAA TAC GAC TCA CTA TAG GGA T
Linear DNA for 23 or 4 bp-RNA membrane, sense strand (92 nt)	Phosphate - ATA GTG AGT CGT ATT ATG CAT CCA ACA ATG AAG TTG ACA TTG AAG TCA TCT GGA CTT CAA GTG CAA CTT CAA TTT GAG GCA ATC CAA TCC CT
Linear DNA for 23 bp-RNA membrane, anti-sense strand (92 nt, 23 bp hybridization with sense strand)	Phosphate - ATA GTG AGT CGT ATT ACA TCA TGA TCA TGA TCA TGA GTG CAC TTG AAG TCC AGA TGA CTT GCA AGA TCA TGA GTT CTT TCA GAG TGA TCC CT
Linear DNA for 4 bp-RNA membrane, anti-sense strand (92 nt, 4 bp hybridization with sense strand)	Phosphate - ATA GTG AGT CGT ATT ACA TCA TGA TCA TGA TCA TGA GAA GCT GAC ATC ATC ATG TGC TCA GCA AGA TCA TGA GTT CTT TCA GAG TGA TCC CT



**Table S4.** DNA sequences for fabricating CpG-DNAPs. DNA sequences for hybridization with primer DNA to form circular DNA are shown in orange. CpG sites for CpG-DNAPs are shown in red.

DNA strands (Length)	Sequence (5'– 3')
Primer DNA (22 nt)	GCC AAA CAT GAA ACT ACA TTC C
Linear DNA for CpG-DNAP sense strand (92 nt)	Phosphate - TAG TTT CAT GTT TGG CTA CTC TAC TTA GAT TAA CGT CAG GAA CGT CAT GGA CTG AGT ACT TAG ATT AAC GTC AGG AAC GTC ATG GAG GAA TG
Linear DNA for CpG-DNAP anti-sense strand (92 nt)	Phosphate - TAG TTT CAT GTT TGG CAA TCT AAG TAC TCA GAA CGT CAG GAA CGT CAT GGA AAT CTA AGT AGA GTA AAC GTC AGG AAC GTC ATG GAG GAA TG

### **Supplementary movie legends**

Movie S1. Representative movie reconstructed from confocal microscopy images showing multi-layered RMMNs assembled with two different RNA membranes.

Movie S2. Representative movie reconstructed from confocal microscopy images showing the transferred RNA membrane (Red) in porcine skin after the RMMN treatment.

## References

1. 3D Systems, <https://ko.3dsystems.com/sites/default/files/2018-11/3d-systems-proJet-mjp-3600-plastic-tech-specs-a4-us-2018-11-08-web.pdf>, (accessed December 2019).